GAS5 regulates diabetic cardiomyopathy via miR-221-3p/p27 axis-associated autophagy

DEZHI CHEN and MIN ZHANG

Department of Endocrinology, Yongchuan Hospital of Chongqing Medical University, Chongqing 402160, P.R. China

Received April 30, 2020; Accepted September 7, 2020

DOI: 10.3892/mmr.2020.11774

Abstract. Diabetic cardiomyopathy (DCM) is one of the primary complications of the cardiovascular system due to diabetes-induced metabolic injury. The present study investigated the autophagy-associated regulatory mechanisms of long non-coding RNAs in cardiac pathological changes in diabetes mellitus (DM). Streptozotocin (STZ)-induced diabetic rats were intramyocardially injected and high concentration glucose (HG)-processed H9C2 cells were infected with growth arrest specific transcript 5 (GAS5)-loaded AAV-9 adenovirus. HG-processed H9C2 cells also underwent transfection with small interfering RNA-p27. Hematoxylin and eosin and Masson staining evaluated myocardial histological changes. Quantitative PCR detected the expression levels of GAS5, fibrosis markers (collagen I, collagen III, TGF-β and connective tissue growth factor) and microRNA (miR)-221-3p. Western blotting determined the expression levels of autophagy-associated proteins [microtubule-associated proteins 1A/1B light chain 3B (LC3B) I, LC3B II and p62] and p27. Targetscan7.2 was used to predict binding sites between miR-221-3 and p27. Dual luciferase reporter assayed the effect of miR-221-3p on luciferase activity of GAS5 and p27. GAS5 downregulated high blood glucose concentrations in STZ-induced diabetic rats, however its expression levels decreased in both HG-processed H9C2 cells and the myocardium of DM model rats. GAS5 attenuated the histological abnormalities and reversed the decreased LC3B II and increased p62 expression levels of DM model rats. miR-221-3p mimic suppressed the activity of both GAS5-wild-type (WT) and p27-WT. miR-221-3p expression levels were increased in both HG-processed H9C2 and diabetic myocardium. p27 expression levels decreased following HG but were upregulated by GAS5. sip27 abolished the effect of GAS5 on DCM. GAS5 promoted cardiomyocyte autophagy in DCM to attenuate myocardial injury via the miR-221-3p/p27 axis.

Correspondence to: Dr Dezhi Chen, Department of Endocrinology, Yongchuan Hospital of Chongqing Medical University, 439 Xuanhua Road, Yongchuan, Chongqing 402160, P.R. China
E-mail: dezhic_chendz@163.com

Abbreviations: lncRNA, long non-coding RNA; DM, diabetes mellitus; STZ, streptozotocin; HG, high concentration glucose

Key words: growth arrest specific transcript 5, diabetes, diabetic cardiomyopathy, autophagy, apoptosis, microRNA-221-3p, p27

Introduction

Diabetic cardiomyopathy (DCM) is a cardiovascular complication of a major chronic metabolic disease, diabetes mellitus (DM) (1), and affects ~12% of patients with DM in Greece (2). In diabetes, myocardial structure alterations, namely left ventricular hypertrophy and functional changes in systole and diastole, emerge and trigger extensive metabolic perturbation (3). The resulting metabolic perturbations manifest as hyperglycaemia, augmented lipid metabolism, hyperlipidaemia and hyperinsulinaemia, impaired cardiac contractility and increased cardiomyocyte dysfunction, injury and cell death, which are all indicative of the development of DCM (4). The physical change in diabetic myocardium is characterized by cardiac hypertrophy, primarily posed by increased left ventricular hypertrophy and is accompanied by decreased systolic and diastolic function (5). Altered diastolic function is considered to be an early sign of diabetic myocardium injury, whereas systolic function alteration may appear in the later stage of injury. Eventually, patients with diabetes develop a high risk of heart failure, with clinical trails reporting a 19-26% incidence rate worldwide (6,7).

Hyperglycaemia is considered to be the primary pathogenic factor of DCM, although the driver of DCM is multifactorial (8). High concentration glucose (HG)-induced hyperglycaemia can cause oxidative burst, which activates maladaptive signaling to further disrupt cellular environmental homeostasis (8). Interactions between numerous molecular mechanisms are implicated in the diabetic myocardium, such as increased concentration of pro-inflammatory cytokines, increased numbers of apoptotic and necrotic cells, fibrosis, mitochondrial dysfunction, oxidative stress, autophagy and altered expression level patterns of microRNAs (miRNAs or miRs) (4). Notably, miRNAs can impose a memory effect related to their altered expressions, which are induced by certain mechanisms in the diabetic heart, and fail to be normalized by glycemic control (9). Therefore, the interplay of

miRNA expression levels and other molecular mechanisms in the diabetic heart needs to be further investigated.

Long non-coding RNAs (lncRNAs) are defined as ncRNAs comprising >200 nucleotides in length, without protein-coding capacity. They have been discovered to participate in multiple physiological and pathological processes via modulating gene transcription, sequestering RNA-binding proteins and sponging miRNAs (10). Emerging evidence has revealed that lncRNAs modulate autophagy by acting as a competing endogenous RNA to sponge miRNA (11,12). The regulatory role of lncRNAs in the pathogenesis of cardiovascular disease has recently been highlighted (13). Hence, the present study aimed to elucidate the mechanism of certain lncRNAs in the development of DCM and its association with cardiac autophagy.

Growth-arrest specific transcript 5 (GAS5) is an lncRNA in the 5'-terminal oligopyrimidine (TOP) class, with the capacity to regulate cell growth, survival and proliferation (14,15). GAS5 serves as the host gene of small nucleolar RNAs (snoRNAs); encoded snoRNAs in the introns of GAS5 have been predicted to function in the 2'-*O*-methylation of ribosomal RNA (16). The 5' TOP sequence involves protein synthesis and the mTOR pathway partly controls translation of 5'-TOP RNAs (17) and influences the RNA expression levels of GAS5 (16). The GAS5 expression levels in serum of patients with diabetes have been demonstrated to decrease, with GAS5 values <10 ng/μl raising the risk of diabetes twelve-fold (18). The present study established a rat model of DM and generated a HG-processed cardiomyocyte environment to compare the performance of GAS5 *in vitro* and *in vivo* and investigated the mechanism underlying GAS5 interactions with its targeted miRNA in DCM to identify potential methods for cardiovascular risk mitigation in DM.

Materials and methods

Ethics statement. All animal experiments were performed in accordance with the guidelines for the Care and Use of Laboratory Animals (19). The present study was approved by the Committee of Experimental Animals of Yongchuan Hospital of Chongqing Medical University (approval no. YHC20190537). Every effort was made to minimize pain and discomfort to the animals. The animal experiments were performed at Yongchuan Hospital of Chongqing Medical University.

Cell culture. H9C2 cells [H9c2 (2-1); The Cell Bank of Type Culture Collection of Chinese Academy of Sciences] were cultured in DMEM [cat. no. 30-2002; American Type Culture Collection (ATCC)] with 10% FBS (cat. no. 30-2020; ATCC) at 37˚C and a pH of 7.2-7.4 in 5% CO_2. A total of 1 ml pancreatic enzyme (cat. no. P816199-50g; Casmart) was added to $1x10^6$ cells for digestion; digestion was stopped by adding cells to DMEM containing 10% FBS. Cells were centrifuged at 1,000 x g for 5 min at 37˚C and maintained at 5% CO_2 at 37˚C for subsequent experiments.

293A cells (293A; BioVector NTCC, Inc.) were cultured in DMEM with 10% FBS and Penicillin-Streptomycin antibiotics (cat. no. P4333; Sigma-Aldrich; Merck KGaA) and sub-cultured in HG DMEM in 5% CO_2 at 37˚C for virus packaging and dual luciferase reporter assay.

Vector construction and adeno-associated virus (AAV-9A) packaging. A certain segment of GAS5 nucleotide sequence (lnc6160405085202-1-5; Guangzhou RiboBio Co., Ltd.) was subcloned into pHBAd (Hanbio Biotechnology Co., Ltd.). Scrambled-small interfering (si)RNA (siG141112151026-1-5; Guangzhou RiboBio Co., Ltd.) was used as a control. 293A cells were co-transfected with 50 ng pHBAd containing the segment of GAS5 nucleotide sequence and pBHGlox (Δ) E1, 3Cre for 6 h using LipoFiter3 transfection reagent (both Hanbio Biotechnology Co., Ltd.). Virus in the cell supernatant, which was obtained via centrifugation at 3,000 x g at 37˚C for 15 min, was precipitated using PEG8000 (cat. no. 07164; Sigma Aldrich; Merck KGaA), harvested and purified via the iodixanol method (20). Virus titer was detected by quantitative (q)PCR (21). Vector construction and virus (AAV-9A) packaging were performed by Hanbio Biotechnology Co., Ltd. The acquired virus was used for rat myocardium injection and H9C2 transfection.

Establishment of diabetic rats. A total of 40 6-week-old male rats (Slac:SD; weight, 160-180 g; Shanghai SLAC Animal Laboratory Co., Ltd.) were kept at 21-22˚C, 50-70% humidity and 12/12-h day/night cycle in a specific pathogen-free environment, with free access to food and water.

Streptozotocin (STZ) used to induce diabetes was procured from Sigma Aldrich (cat. no. 572201; Merck KGaA) and 60 mg/kg/day of STZ was dissolved in 10 mM citrate buffer (pH, 4.5; cat. no. A55926-500ml; Casmart) to prepare STZ injection. The rats were randomly distributed into the following four groups (n=10/group): Control (rats with no injection), DM (rats injected with STZ), DM + NC (rats injected with STZ and AAV-9 containing scrambled-siRNA) and DM + GAS5 (rats injected with STZ and AAV-9 containing GAS5 nucleotide sequence). In the latter three groups, rat myocardium was intraperitoneally injected with prepared STZ for 5 consecutive days, in the presence or absence of injection of 100 μl AAV-9 containing scrambled-RNA or GAS5 nucleotide sequence. Following injection, the rats were maintained in the aforementioned conditions. On the 7th day after the final injection, the caudal vein blood glucose concentration and body weight of rats were measured; blood glucose level >16.7 mmol/l was considered to indicate a diabetic rat.

Reverse transcription-qPCR. mRNA was extracted using a TRIzol Plus RNA Purification kit (cat. no. 12183555; Thermo Fisher Scientific, Inc.) according to the manufacturer's instructions. A total of 50-100 ml myocardium from one rat was lysed using TRIzol reagent (1 ml) to retain the lysate of mRNA. Then, 0.2 ml chloroform (cat. no. 48520-U; Sigma Aldrich; Merck KGaA) was used to extract the lysate. The lysate was centrifuged (12,000 x g) for 15 min at 4˚C, then an equal volume of 70% ethanol (cat. no. 459836; Sigma-Aldrich; Merck KGaA) was added and mixed well by vortex. miRNA was lysed and extracted using an RNAmisi microRNA kit (cat. no. 110501; Beijing BLKW Biotechnology Co., Ltd.). Following isolation of the precipitate from the supernatant, 75% ethanol was used to resuspend the precipitate. The precipitate underwent 7,500 x g centrifugation for 10 min at 4˚C and was then dissolved in 20 μl diethyl pyrocarbonate

Table I. Primers for quantitative PCR detection of genes.

Gene	Sense (5'→3')	Antisense (5'→3')
Growth arrest specific transcript 5	AGCCAGAAAATGGGATGGTGG	ACTGCACTGTCCACTTGTCA
GAPDH	CAATGACCCCTTCATTGACC	GACAAGCTTCCCGTTCTCAG
p62	TCAGTTAAAGCCCCGGAAGA	AACAACCTCTAGCTCCACCC
Collagen I	GCTCCTCTTAGGGGCCACT	CCACGTCTCACCATTGGGG
Collagen III	CTGTAACATGGAAACTGGGGAAA	CCATAGCTGAACTGAAAACCACC
TGF-β	CTCCCGTGGCTTCTAGTGC	GCCTTAGTTTGGACAGGATCTG
Connective tissue growth factor	GGGCCTCTTCTGCGATTTC	ATCCAGGCAAGTGCATTGGTA
LC3B I/II	ATGGTAGTCTGTGGTGGTGG	CATACCTTGAATCCCAGCGC
Rno-microRNA-221-3p	A(24)CACTGTCATGCCGTTACGTAG CGTATCGTTGACAGCTAACCAA	GCTGTCAACGATACGCTACGTAACG
U6	CTCGCTTCGGCAGCACA	AACGCTTCACGAATTTGCGT

LC3B, microtubule-associated proteins 1A/1B light chain 3B.

(cat. no. rats (Slac:SD). cDNA for mRNA was produced using a First Strand cDNA Synthesis kit (cat. no. K1621, Thermo Fisher, Inc.) and the following temperature protocol: 65˚C for 5 min, 42˚C for 60 min and 70˚C for 5 min, according to the manufacturer's instructions. cDNA for miRNA was produced using a TaqMan MicroRNA Reverse Transcription kit (Applied Biosystems; Thermo Fisher Scientific, Inc.). The cDNA was transferred to an Applied Biosystems 7500 FAST real-time PCR machine (Applied Biosystems; Thermo Fisher Scientific, Inc.) for PCR using IV One-Step RT-PCR System with ezDNase (cat. no. 12595025; Thermo Fisher Scientific, Inc.). The following thermocycling conditions were used for qPCR: 95˚C for 10 min; and 35 cycles of 95˚C for 15 sec and 60˚C for 60 sec. The sense and antisense primers are listed in Table I. Fold change in the expression levels of mRNA and miRNA was determined using the $2^{-\Delta\Delta Cq}$ method (22).

Hematoxylin and eosin (H&E) staining. In order to observe rat myocardium and calculate cardiomyocyte cross-sectional area (CSA), rat myocardium (thickness, 0.3 cm) was fixed in 10% formalin at 37˚C for 24 h (cat. no. HT5011; Sigma-Aldrich; Merck KGaA), dehydrated by ethanol, blocked by paraffin (cat. no. 1.07150; Sigma-Aldrich; Merck KGaA) and sliced (5-μm thick). Later, the sliced rat myocardium was dewaxed by soaking in xylene (cat. no. X749400-250g; Casmart) twice (5 min each). Rehydration was performed via soaking in gradient ethanol (100, 95, 85 and 75%; 2 min each) and rinsing with water. The cells were stained with 5% hematoxylin (cat. no. H9627-100G; Casmart) at 37˚C for 15 min, then soaked in 5% acetic acid (cat. no. A465500; Casmart) to be differentiated and soaked in distilled water for 20 min to develop blue. Then, the cells were stained by 0.5% eosin (cat. no. 170; Casmart) at 37˚C for 10 min, then rinsed with distilled water at 37˚C for 2 sec. Dehydration was performed with graded ethanol (75%, 1 min; 85%, 1 min; 90%, 1 min; 100%, 2 min; and 100%, 4 min). Cells were soaked in xylene twice (5 min each), then sealed by neutral resin (cat. no. XY-23474-1; Casmart) at 37˚C for 2 h for observation using a light microscope (CX43; Olympus Corporation).

Masson staining. Rat myocardium was stained using a Masson staining kit (cat. no. G1340; Beijing Solarbio Science & Technology, Co., Ltd.) according to the manufacturer's instructions for collagen volume fraction calculation. Rat myocardium was dewaxed by soaking in xylene twice (10 min each). Weigert dye solutions A and B were mixed at a ratio of 1:1 to prepare Weigert Iron hematoxylin dye solution. Myocardium was stained with Weigert Iron hematoxylin solution at 37˚C for 10 min and differentiated by acidic ethanol for 10 sec. Masson solution was used to develop blue on the myocardium. Then, 10% porcelain Red Magenta solution was used to stain the myocardium at 37˚C for 10 min. The myocardium underwent sequential weak and phosphomolybdic acid washes. Myocardium was immersed in aniline blue solution at 37˚C for 2 min, then dehydrated with anhydrous ethanol and soaked in xylene three times. Finally, the myocardium was blow-dried and sealed and tissue observation was performed using a light microscope (CX43; Olympus Corporation).

Western blot. A total of 250 mg rat myocardium was homogenized using 1 ml ice cold RIPA buffer (cat. no. P0013B; Beyotime Institute of Biotechnology). Following homogenization, total protein was extracted. Measurement of protein concentration was conducted using a BCA Protein Assay kit (cat. no. 23225; Thermo Fisher Scientific, Inc.). The obtained protein (20 μl per lane) and protein marker (10-170 kD) were subjected to gel electrophoresis with 12% SDS-PAGE (cat. no. P0012A; Beyotime Institute of Biotechnology). Following electrophoresis, the protein was transferred to nitrocellulose membranes (cat. no. N8395; Sigma Aldrich; Merck KGaA). Following blocking in TBS with 1% Tween-20 (TBST; cat. no. TA-125-TT; Thermo Fisher Scientific, Inc.) at 37˚C for 1 h, the membrane was incubated with primary antibody at 4˚C overnight and subsequently incubated with HRP-conjugated secondary antibody for 1 h at room temperature. The protein was transferred to an ECL system (Amersham Pharmaci; Cytiva) with ECL reagent (EMD Millipore). ImageJ software 1.50 (National Institutes of Health) was utilized to analyze the optical density of protein bands. The following primary antibodies (all Abcam) were used: Rabbit Anti-p27 KIP 1 (27 kD;

Table II. Change in body weight and blood glucose of STZ-induced diabetic rats.

	Body weight, g		Blood glucose, mmol/l	
Group	Pre-STZ	Day 7 post-STZ	Pre-STZ	Day 7 post-STZ
Control	142.36±3.62	181.60±5.07[a]	5.63±0.52	5.71±0.42
DM	144.28±3.96	153.42±5.42[a]	5.66±0.42	23.67±2.92[a]
DM + negative control	140.66±4.32	152.71±4.66[a]	5.68±0.45	23.74±3.07[a]
DM + growth arrest specific transcript 5	146.33±5.02	154.55±5.02[a]	5.73±0.58	20.45±2.82[a]

[a]P<0.001 vs. control. STZ, streptozotocin; DM, diabetes mellitus.

1:5,000; product code ab32034), Mouse Anti-GAPDH (36 kD; 1:1,000; product code ab8245), Mouse Anti-SQSTM1/p62 antibody (62 kD; 1:1,000; product code ab56416) and Rabbit Anti-LC3B I/LC3BII antibody (19 and 17 kD, respectively; 1:1,000; product code ab48394). The following secondary antibodies were used: Goat Anti-Rabbit IgG H&L (HRP) and Goat Anti-Mouse IgG H&L (HRP) (both 1:5,000; product codes ab205718 and ab205719, respectively; both Abcam).

Luciferase reporter assay. Online databases starBase (version 2.0; starbase.sysu.edu.cn/agoClipRNA.php?source=lncRNA) and Targetscan7.2 (targetscan.org/vert_72/) were used to predict potential binding sites of miR-221-3p on GAS5 and p27. The 3'-untranslated region (3'-UTR) of GAS5 (5'-AUUCUGCAU UCCCAUGUAGC-3') and p27 wild-type (WT) (5'-CUCUAA AAGCGUUGGAUGUAGCA-3') containing the potential miR-221-3p binding sites were cloned into pRL-CMV luciferase reporter plasmid (cat. no. E2261; Promega Corporation). The mutant (MUT) sequence (GAS5, 5'-CUUAUCGUUUCGCCC ACGUA-3'; p27, 5'-CUCUAAACCAGUUGGCAUAGAUA-3') was used as the MUT control. The 293A cells were co-transfected with the luciferase reporter plasmid and miR-221-3p mimic (miR10000278-1-5; Guangzhou RiboBio Co., Ltd.) or mimic control using Lipofectamine® 2000 (cat. no. 11668019; Thermo Fisher Scientific, Inc.) according to the manufacturer's instructions. At 48 h post-transfection, firefly luciferase activity was normalized to *Renilla* luciferase activity, and detected using Promega Dual Luciferase Reporter Assay System (Promega Corporation), according to manufacturer's instructions.

Transfection of sip27. sip27 (sense, 5'-UGGAUUUGUACC AUUCUUCUG-3' and antisense, 5'-GAAGAAUGGUACAAA UCCAAG-3') (cat. no. 12324; Cell Signaling Technology, Inc.), miR-221-3p mimic (miR10000890-1-5; Guangzhou RiboBio Co., Ltd.) and mimic control were transfected into H9C2 cells using Lipofectamine® 2000 Transfection Reagent (cat. no. 11668019; Thermo Fisher Scientific, Inc.) according to the manufacturer's instructions. A total of $1x10^4$ H9C2 cells were seeded to reach 70-90% confluence per well in a 96-well plate (cat. no. 14-245-101; Thermo Fisher Scientific, Inc.). Lipofectamine reagent (1 μl) was diluted in Opti-MEM (25 μl) (cat. no. 31985062; Thermo Fisher Scientific, Inc.). Then, 2.5 μg (0.5 μg/μl) RNA of interest was diluted in 125 μl Opti-MEM. The diluted RNA was mixed 1:1 with diluted Lipofectamine and incubated at room temperature for 5 min. Following incubation, 10 μl RNA-lipid complex, 100 ng final RNA and 0.5 μl Lipofectamine were added per well and again incubated at 37˚C for 3 days.

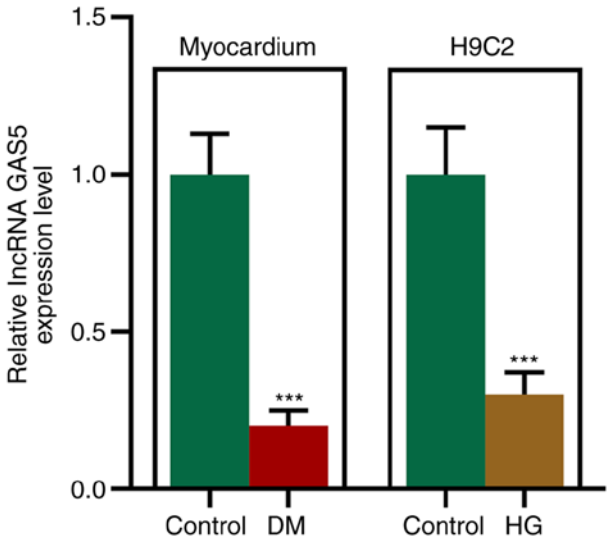

Figure 1. GAS5 expression levels are decreased in the myocardium of STZ-induced diabetic rats and HG-processed H9C2 cells. Quantitative PCR analyzed GAS5 expression levels. GAPDH acted as the internal control. ***P<0.001 vs. Control. GAS5, growth arrest specific transcript 5; STZ, streptozotocin; HG, high concentration glucose; DM, diabetes mellitus; lncRNA, long non-coding RNA.

Statistical analysis. Data are presented as the mean ± SEM of three independent repeats. One-way ANOVA was used to compare multiple groups, followed by post hoc Tukey's test. An unpaired Student's t-test was used to analyze the differences between two groups. P<0.05 was considered to indicate a statistically significant difference.

Results

GAS5 expression levels are decreased in the myocardium of STZ-induced diabetic rats and HG-processed H9C2 cells. At the start of the experiment, there was no notable association between rat body weight and blood glucose levels (Table II). However, on day 7 after STZ injection, the body weight in the DM, DM + GAS5 and DM + NC groups

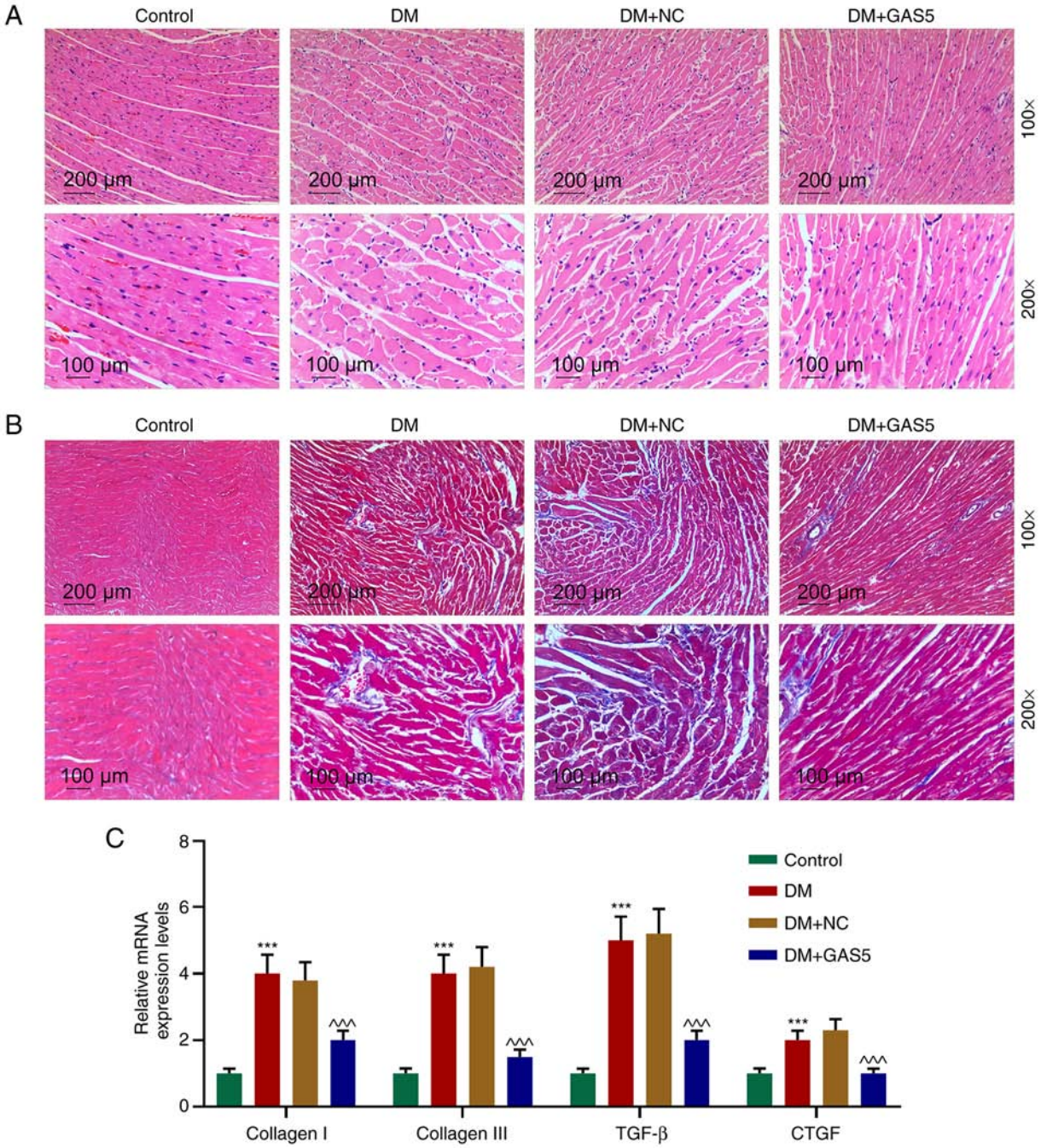

Figure 2. GAS5 improves histological abnormalities in diabetic rats. (A) Histological abnormalities in STZ-induced diabetic myocardium were observed via hematoxylin eosin staining. (B) Masson staining assessed fibrosis of STZ-induced diabetic myocardium. (C) Quantitative PCR detected the expression levels of fibrosis markers (collagen I, collagen III, TGF-β and CTGF). GAPDH served as an internal reference. ***P<0.001 vs. Control; ^^^P<0.001 vs. DM + NC. GAS5, growth arrest specific transcript 5; STZ, streptozotocin; CTGF, connective tissue growth factor; DM, diabetes mellitus; NC, negative control.

exhibited a significant decrease, compared with the control group (Table II). Moreover, the blood glucose concentration in these three groups increased to >16.7 mM 7 days after STZ injection (Table II). It was confirmed that STZ successfully established a DM model in rats, as the blood glucose increased and body weight decreased following STZ injection (Table II). GAS5 was significantly downregulated in the myocardium of diabetic rats and HG-processed H9C2 cells. GAS5 expression levels in STZ-induced diabetic rats were decreased, which was similar to that in HG-processed cardiomyocytes (Fig. 1).

GAS5 improves histological abnormalities in diabetic rats. H&E staining was utilized to measure the CSA of cardiomyocytes in diabetic rats. The results demonstrated typical histological abnormalities (23), including cardiomyocyte hypertrophy, myocardial fiber breakage and increased intercellular space in diabetic rats, whereas GAS5 ameliorated these abnormalities (Fig. 2A). As fibrosis is a biological feature of DCM, which manifests in collagen accumulation in myocardium (24), the extent of fibrosis was determined based on collagen volume observation via Masson staining, calculation of collagen volume fraction and fibrosis marker detection

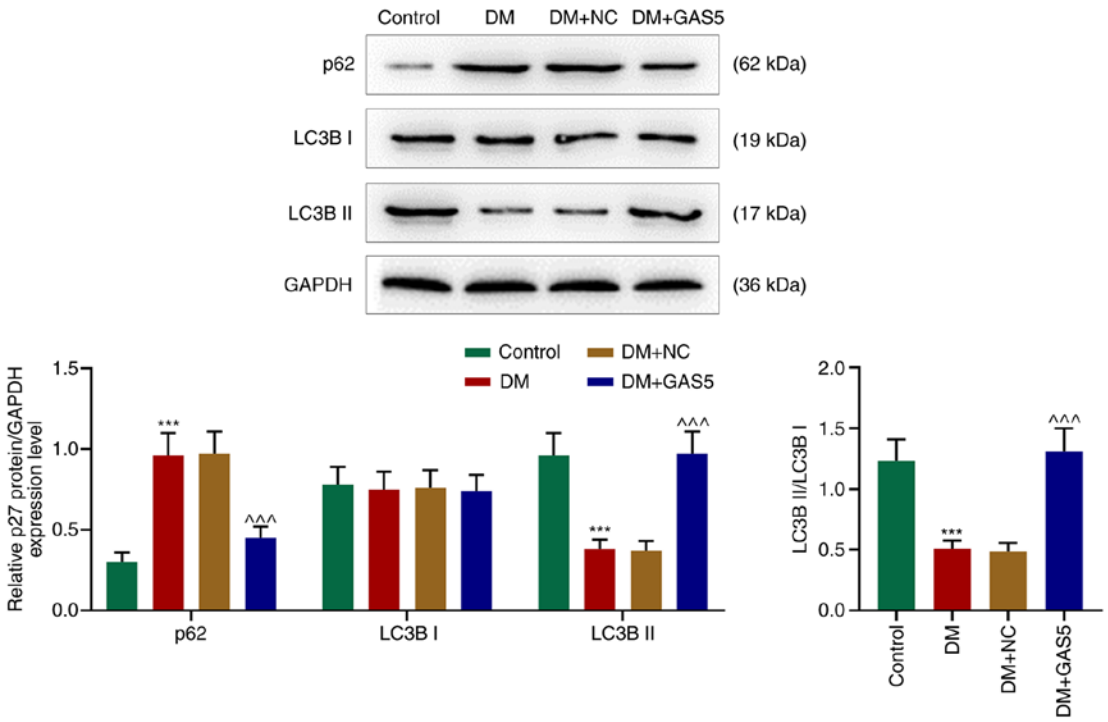

Figure 3. GAS5 reverses inhibition of autophagy in the myocardium of diabetic rats. Western blotting evaluated the protein expression levels of p62, LC3B I and LC3B II in the myocardium of diabetic rats. GAPDH was used as an internal control and the ratio of LC3B II/LC3B I was calculated. ***P<0.001 vs. Control; ^^^P <0.001 vs. DM + NC. GAS5, growth arrest specific transcript 5; LC3B, microtubule-associated proteins 1A/1B light chain 3B; DM, diabetes mellitus; NC, negative control.

by qPCR (Fig. 2B and C). Myocardial fibrosis was increased in diabetic rats, but notably relieved by GAS5 (Fig. 2B). Expression levels of fibrosis markers (collagen I, collagen III, TGF-β and connective tissue growth factor) were significantly increased in the myocardium in DM, indicating synthesis of collagen and significant growth of connective tissue, whereas the expression levels were inhibited by GAS5 (Fig. 2B and C). The results indicated that GAS5 alleviated diabetes-induced myocardial histological abnormalities and fibrosis (Fig. 2).

GAS5 reverses inhibition of autophagy in the myocardium of diabetic rats. In order to investigate the role of GAS5 in cardiac autophagy in diabetic rats, LC3B I, LC3B II and p62 expression levels were measured using western blotting. p62 levels were increased in the myocardium of diabetic rats, however LC3B I remained stable, LC3B II and the ratio of LC3B II/LC3B I were decreased, demonstrating a reduction in the formation of autophagosomes and suppressed degradation of autophagosomes, which further indicated inhibited cardiac autophagy in diabetic rats (Fig. 3). GAS5 counteracted DM-induced autophagy inhibition, which was demonstrated by an increased ratio of LC3B II/LC3B I and decreased p62 expression levels, suggesting that GAS5 reversed the inhibitory effect of DM on cardiac autophagy (Fig. 3).

GAS5 competitively binds miR-221-3p, which is upregulated in the myocardium of diabetic rats and HG-processed H9C2 cells, to increase p27 in HG-processed H9C2 cells. In order to determine the internal mechanism by which GAS5 promotes autophagy, starBase was employed to predict the potential binding site between miR-221-3p and GAS5 as well as miR-221-3p and p27. GAS5-WT had binding sites with miR-221-3p and mutual binding sites between miR-221-3p and p27 were identified at position 201-208 of the p27-WT 3'UTR (Fig. 4A and D). Regulatory associations between mutual binding sites were assessed via luciferase reporter assay. The expression levels of GATS5-WT and p27-WT were negatively regulated by miR-221-3p mimic, however the MUT expression levels were unaffected (Fig. 4B and E).

The expression levels of miR-221-3p were significantly increased in the myocardium of diabetic rats as well as in HG-processed H9C2 cells, whereas the protein expression levels of p27 were decreased in a HG environment (Fig. 4C and F). Notably, GAS5 reversed this inhibition of p27 protein expression levels, which may be due to GAS5 competitively binding to miR-221-3p, preventing p27 binding to miR-221-3p and thus increasing p27 protein expression levels (Fig. 4F). Moreover, transfection of sip27 significantly counteracted the effect of GAS5, resulting in low protein expression levels of p27 (Fig. 4F) in a HG environment.

Sip27 reverses the facilitating effect of GAS5 on HG-inhibited autophagy in HG-processed H9C2 cells. Similar to the impact of GAS5 on the myocardium of diabetic rats, the significantly upregulated p62 expression levels in HG-processed H9C2 cells was downregulated by GAS5, whereas LC3B II expression levels were decreased in HG-processed H9C2 cells but increased following exposure to GAS5 (Fig. 5). Similarly, the ratio of LC3B II/LC3B I was decreased in HG-processed H9C2 cells, whereas this effect was reversed by GAS5 (Fig. 5). The addition of sip27 counteracted the effects of GAS5 on the

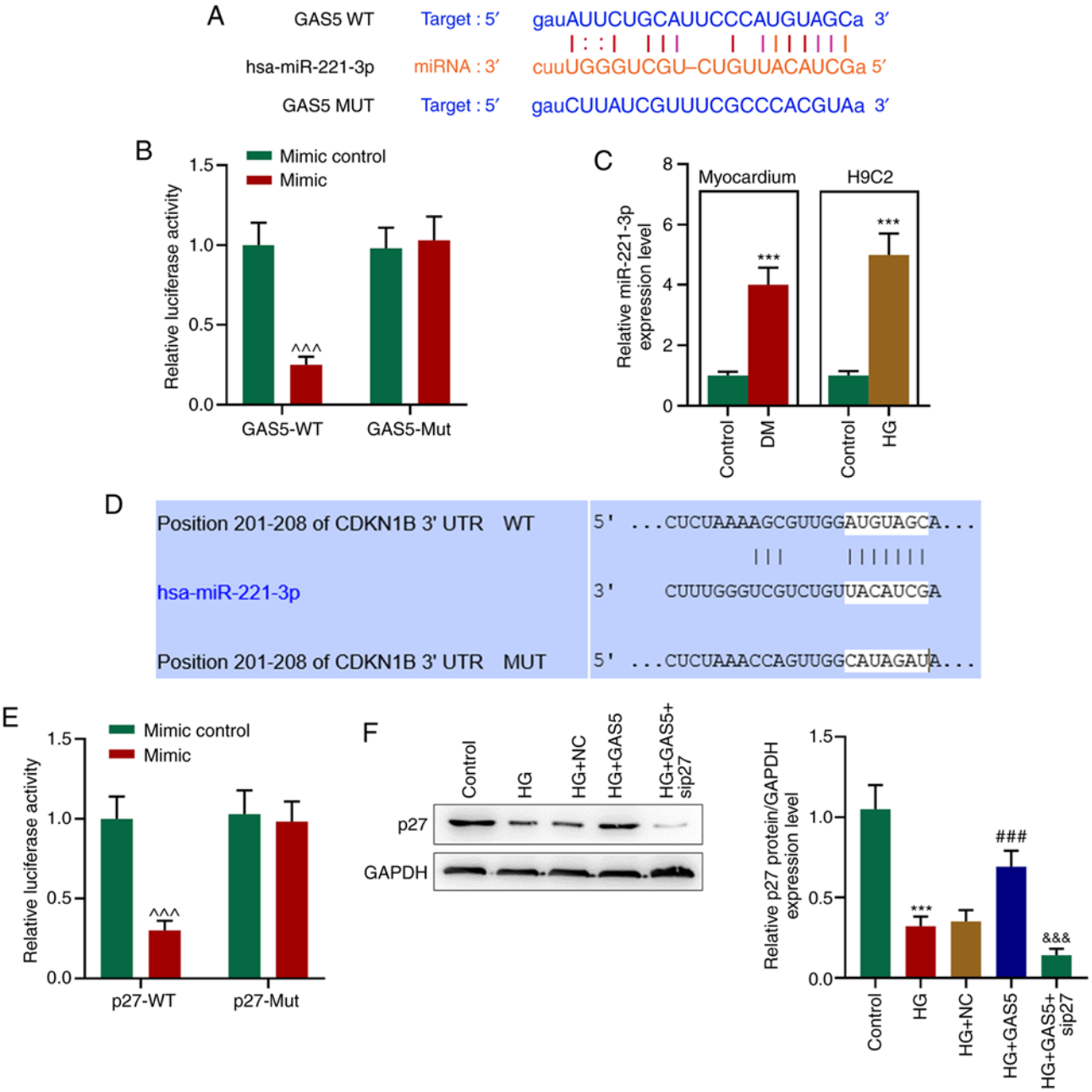

Figure 4. GAS5 competitively binds miR-221-3p, which is increased in the myocardium of diabetic rats and HG-processed H9C2 cells, to increase p27 in HG-processed H9C2 cells. (A) starBase predicted binding sites between GAS5 and miR-221-3p. (B) Dual luciferase reporter assay assessed the effect of miR-221-3p mimic on the activity of GAS5. (C) miR-221-3p expression levels in the myocardium of diabetic rats and HG-processed H9C2 cells were assessed via quantitative PCR. U6 was used as a reference gene. (D) Targetscan7.2 predicted binding sites between miR-221-3p and p27. (E) Dual luciferase reporter assayed the effect of miR-221-3p mimic on the activity of p27. (F) Western blotting examined the protein expression levels of p27 in HG-processed H9C2 cells. GAPDH was used as a reference gene. ***P<0.001 vs. Control; $^{\wedge\wedge\wedge}$P <0.001 vs. mimic control; $^{\#\#\#}$P<0.001 vs. HG + NC; $^{\&\&\&}$P<0.001 vs. HG + GAS5. GAS5, growth arrest specific transcript; miR, microRNA; HG, high concentration glucose; NC, negative control; WT, wild-type; MUT, mutant; UTR, untranslated region; si, small interfering.

expression levels of p62 and LC3B II, ratio of LC3B II/LC3B I and cardiomyocyte autophagy.

Discussion

The key role of lncRNAs in the regulation of diverse types of cardiovascular physio-pathology processes, including atherosclerosis, coronary disease, cardiac remodeling and heart failure, has been recorded (25-28) and its involvement in the pathogenesis of DCM, an important cardiovascular complication of diabetes, has previously been investigated (29). lncRNA KCNQ1 opposite strand/antisense transcript 1 has been revealed to mediate pyroptosis in DCM via affecting miR-214-3p expression levels (30). lncRNAs H19 and myocardial infarction-associated transcript have been revealed to influence cardiomyocyte apoptosis via regulating their target miRNAs in DCM (31,32). lncRNA HOX transcript antisense RNA (HOTAIR) improved cardiac function, decreased oxidative stress and inflammation and protected myocytes from death in mice with DCM (33).

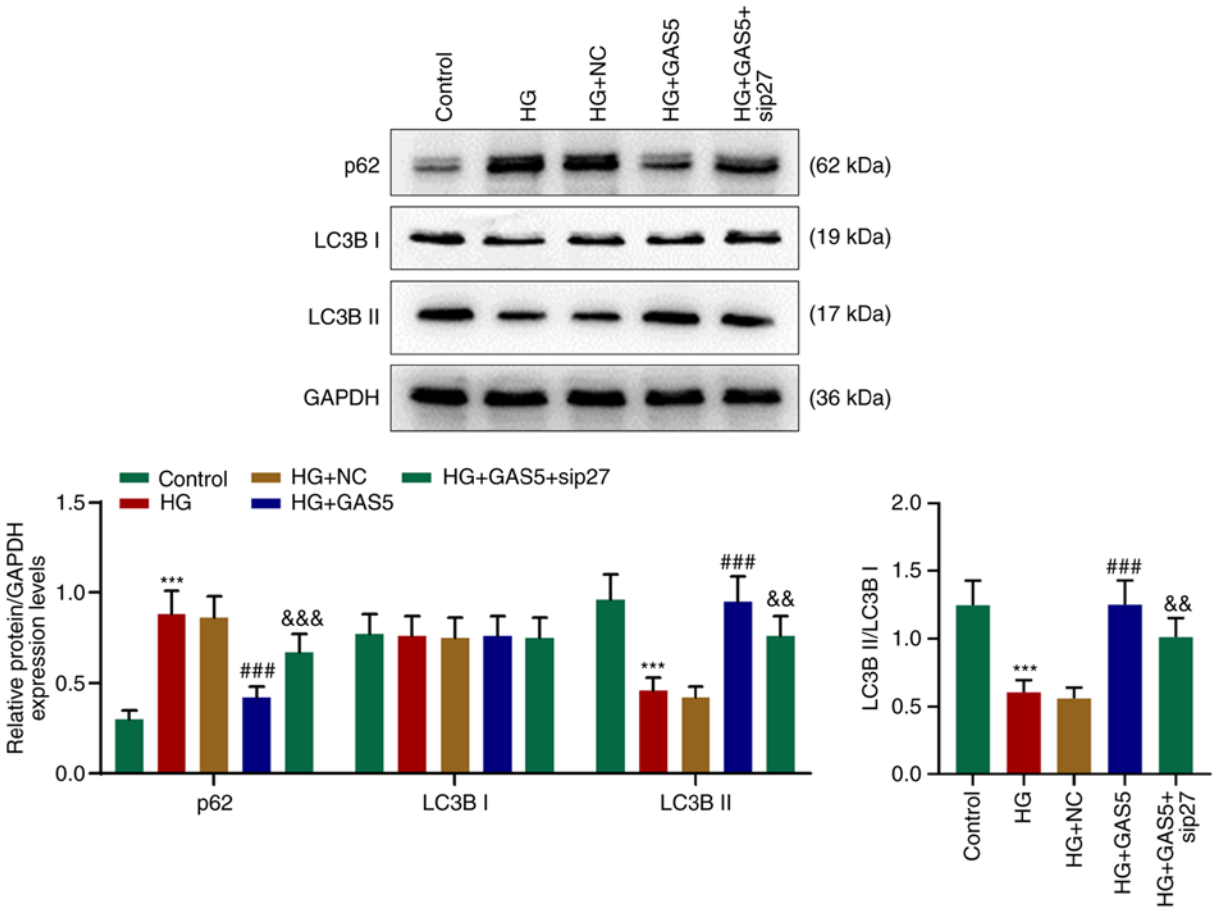

Figure 5. sip27 reverses the facilitating effect of GAS5 on HG-inhibited autophagy in HG-processed H9C2 cells. Western blotting assessed the protein expression levels of p62, LC3B I and LC3B II in HG-processed H9C2 cells. GAPDH was used as an internal reference gene and the ratio of LC3B II/LC3B I was calculated. ***P<0.001 vs. Control; $^{###}$P<0.001 vs. HG + NC; $^{&&}$P<0.01 and $^{&&&}$P<0.001 vs. HG + GAS5. si, small interfering; GAS5, growth arrest specific transcript 5; HG, high concentration glucose; LC3B, microtubule-associated proteins 1A/1B light chain 3B; NC, negative control.

lncRNA GAS5 has been revealed to be aberrantly increased in peripheral blood mononuclear cells (PBMCs) from patients with type 2 diabetes and changes in its expression levels are positively associated with poor glycemic control, insulin resistance and transcriptional markers of senescence and inflammation (34). Thus, it was hypothesized that GAS5 expression levels serve a vital role in the development of the diabetic heart. Furthermore, a previous study demonstrated an association between decreased GAS5 expression levels and diabetes; individuals with absolute GAS5 <10 ng/μl were 12 times more likely to have diabetes (18). Therefore, in order to clarify the mechanism of GAS5 in DCM, STZ-induced diabetic rats and HG-processed H9C2 cells were established. Similar to the results obtained by Tao *et al* (35), STZ injection to rat myocardium resulted in decreased body weight and increased blood glucose concentration, indicating successful establishment of diabetic rats. Contrary to the increased expression levels of GAS5 in PBMCs from patients with type 2 diabetes, the present results revealed decreased expression levels of GAS5 both in the rat myocardium and HG-processed H9C2 cells, suggesting that GAS5 expression patterns differ according to the cell types in patients with DM.

Diabetes induces cardiac metabolic dysregulation that is linked with oxidative stress and autophagy disturbance, which induce cell death, fibrotic 'backfill' (increased fibrosis) and cardiac dysfunction (36). A previous study reported diabetes-induced cardiovascular histological changes, such as increased left ventricular and wall thickness, decreased volume of the left ventricular systolic chamber and increased arterial stiffness (5). The present study further observed enlarged CSA and aggravated fibrosis in the myocardium of diabetic rats, which was consistent with results reported by Gao *et al* (33). Moreover, Gao *et al* also demonstrated that pathological changes (including increased CSA and fibrosis) were reversed by HOTAIR overexpression. The present study demonstrated that GAS5 serves a similar role to HOTAIR in the myocardium of diabetic rats.

Prior studies have demonstrated inhibited cardiac autophagy in diabetic OVE26 mice, as evidenced by decreased LC3-II expression levels, and have observed that enhancement of cardiac autophagy is concomitant with improved cardiac function in DCM (37,38). Lower p62 expression levels are also a sign of inhibited cardiac autophagy in DCM (39). The present study detected decreased LC3-II expression levels and increased p62 expression levels, which reflected inhibition of autophagosome formation in the myocardium of diabetic rats. Moreover, GAS5 in the diabetic myocardium resulted in cardiomyocyte autophagy rebounding, which indicated that GAS5 ameliorates cardiac function of patients with DM patients via promoting autophagy.

miRNA expression levels in diabetic mice have been demonstrated to be significantly altered and do not recover with subsequent normoglycaemia, which may explain why diabetic cardiomyopathy progresses even under normal blood glucose levels; this indicates that glycemic control is not a solution to prevent DCM (9). A previous study demonstrated that lncRNAs function as miRNA sponges to decrease their regulatory effect on mRNAs (40). As lncRNAs also serve a regulatory role, it was hypothesized that GAS5 sponges its direct target miRNA to affect indirectly associated mRNAs and that this may be a solution to control the development of DCM. Previous research indicated that miR-221-3p can bind to the 3'UTR of p27 and the overexpression of miR-221-3p in non-small cell lung cancer was revealed to lower the expression levels of p27, promoting cell cycle progression (41). In the present study, overexpression of miR-221-3p was detected both in the myocardium of diabetic rats and HG-processed H9C2 cells. As anticipated, the expression levels of p27 decreased in HG-processed H9C2 cells. Additionally, an axis of miR-221-3p and p27 was implicated in the regulation of GAS5 in the present study. In order to substantiate the regulatory effect of GAS5 on the miR-221-3p/p27 axis, the present study demonstrated that GAS5-mediated upregulation of p27 and sip27 expression levels offset the effect of GAS5 in HG-processed H9C2. Similarly to the *in vivo* results, autophagy was inhibited in HG-processed H9C2 cells. GAS5 increased autophagy in HG-processed H9C2 cells, but sip27 counteracted this effect. The present results indicated that GAS5 may upregulate p27 via sponging miR-221-3p to promote cardiomyocyte autophagy.

In conclusion, GAS5 reversed the histopathological changes induced by DCM and enhanced cardiomyocyte autophagy to ameliorate myocardial function. The mechanism underlying the effect of GAS5 in the diabetic myocardium may be attributed to a GAS5/miR-221-3p/p27 competing endogenous network and cardiomyocyte autophagy. Thus, GAS5 may promote cardiomyocyte autophagy via regulating the miR-221-3p/p27 axis to protect myocardial function in DCM.

Acknowledgements

Not applicable.

Funding

No funding was received.

Availability of data and materials

The datasets used and/or analyzed during the current study are available from the corresponding author on reasonable request.

Authors' contributions

DC designed the study and wrote the manuscript. MZ performed the research. MZ analyzed the data. All authors contributed to editorial changes in the manuscript. All authors read and approved the final manuscript.

Ethics approval and consent to participate

The present study was approved by the Committee of Experimental Animals of Yongchuan Hospital of Chongqing Medical University (approval no. YHC20190537).

Patient consent for publication

Not applicable.

Competing interests

The authors declare that they have no competing interests.

References

1. Boudina S and Abel ED: Diabetic cardiomyopathy, causes and effects. Rev Endocr Metab Disord 11: 31-39, 2010.
2. Trachanas K, Sideris S, Aggeli C, Poulidakis E, Gatzoulis K, Tousoulis D and Kallikazaros I: Diabetic cardiomyopathy: From pathophysiology to treatment. Hellenic J Cardiol 55: 411-421, 2014.
3. Hayat SA, Patel B, Khattar RS and Malik RA: Diabetic cardiomyopathy: Mechanisms, diagnosis and treatment. Clin Sci (Lond) 107: 539-557, 2004.
4. Bugger H and Abel ED: Molecular mechanisms of diabetic cardiomyopathy. Diabetologia 57: 660-671, 2014.
5. Devereux RB, Roman MJ, Paranicas M, O'Grady MJ, Lee ET, Welty TK, Fabsitz RR, Robbins D, Rhoades ER and Howard BV: Impact of diabetes on cardiac structure and function: The strong heart study. Circulation 101: 2271-2276, 2000.
6. Lüscher TF: Heart failure and comorbidities: Renal failure, diabetes, atrial fibrillation, and inflammation. Eur Heart J 36: 1415-1417, 2015.
7. Jia G, Hill MA and Sowers JR: Diabetic cardiomyopathy: An update of mechanisms contributing to this clinical entity. Circ Res 122: 624-638, 2018.
8. Boudina S and Abel ED: Diabetic cardiomyopathy revisited. Circulation 115: 3213-3223, 2007.
9. Costantino S, Paneni F, Lüscher TF and Cosentino F: MicroRNA profiling unveils hyperglycaemic memory in the diabetic heart. Eur Heart J 37: 572-576, 2016.
10. Moran VA, Perera RJ and Khalil AM: Emerging functional and mechanistic paradigms of mammalian long non-coding RNAs. Nucleic Acids Res 40: 6391-6400, 2012.
11. Liu K, Hou Y, Liu Y and Zheng J: LncRNA SNHG15 contributes to proliferation, invasion and autophagy in osteosarcoma cells by sponging miR-141. J Biomed Sci 24: 46, 2017.
12. Wang K, Liu CY, Zhou LY, Wang JX, Wang M, Zhao B, Zhao WK, Xu SJ, Fan LH, Zhang XJ, *et al*: APF lncRNA regulates autophagy and myocardial infarction by targeting miR-188-3p. Nat Commun 6: 6779, 2015.
13. Sallam T, Sandhu J and Tontonoz P: Long noncoding RNA discovery in cardiovascular disease: Decoding form to function. Circ Res 122: 155-166, 2018.
14. Lander ES, Linton LM, Birren B, Nusbaum C, Zody MC, Baldwin J, Devon K, Dewar K, Doyle M, FitzHugh W, *et al*: Initial sequencing and analysis of the human genome. Nature 409: 860-921, 2001.
15. Amaral PP, Clark MB, Gascoigne DK, Dinger ME and Mattick JS: lncRNAdb: A reference database for long noncoding RNAs. Nucleic Acids Res 39: D146-D151, 2011.
16. Smith CM and Steitz JA: Classification of gas5 as a multi-small-nucleolar-RNA (snoRNA) host gene and a member of the 5'-terminal oligopyrimidine gene family reveals common features of snoRNA host genes. Mol Cell Biol 18: 6897-6909, 1998.
17. Meyuhas O: Synthesis of the translational apparatus is regulated at the translational level. Eur J Biochem 267: 6321-6330, 2000.
18. Carter G, Miladinovic B, Patel AA, Deland L, Mastorides S and Patel NA: Circulating long noncoding RNA GAS5 levels are correlated to prevalence of type 2 diabetes mellitus. BBA Clin 4: 102-107, 2015.
19. Clark JD, Baldwin RL, Bayne KA, Brown MJ, Gebhart GF and Gonder JC: Guide for the care and use of laboratory animals. Institute of Laboratory Animal Resources, Institute of Laboratory Animal Resources Commission on Life Sciences, National Research Council, National Academy Press, Washington, D.C. 1996.

20. Zolotukhin S, Byrne BJ, Mason E, Zolotukhin I, Potter M, Chesnut K, Summerford C, Samulski RJ and Muzyczka N: Recombinant adeno-associated virus purification using novel methods improves infectious titer and yield. Gene Ther 6: 973-985, 1999.
21. Puglia AL, Rezende AG, Jorge SA, Wagner R, Pereira CA and Astray RM: Quantitative RT-PCR for titration of replication-defective recombinant Semliki forest virus. J Virol Methods 193: 647-652, 2013.
22. Pfaffl MW: A new mathematical model for relative quantification in real-time RT-PCR. Nucleic Acids Res 29: e45, 2001.
23. Zhong P, Wu L, Qian Y, Fang Q, Liang D, Wang J, Zeng C, Wang Y and Liang G: Blockage of ROS and NF-κB-mediated inflammation by a new chalcone L6H9 protects cardiomyocytes from hyperglycemia-induced injuries. Biochim Biophys Acta 1852: 1230-1241, 2015.
24. Zhang Y, Zhang YY, Li TT, Wang J, Jiang Y, Zhao Y, Jin XX, Xue GL, Yang Y, Zhang XF, *et al*: Ablation of interleukin-17 alleviated cardiac interstitial fibrosis and improved cardiac function via inhibiting long non-coding RNA-AK081284 in diabetic mice. J Mol Cell Cardiol 115: 64-72, 2018.
25. Uchida S and Dimmeler S: Long noncoding RNAs in cardiovascular diseases. Circ Res 116: 737-750, 2015.
26. Shen S, Jiang H, Bei Y, Xiao J and Li X: Long non-coding RNAs in cardiac remodeling. Cell Physiol Biochem 41: 1830-1837, 2017.
27. Greco S, Zaccagnini G, Perfetti A, Fuschi P, Valaperta R, Voellenkle C, Castelvecchio S, Gaetano C, Finato N, Beltrami AP, *et al*: Long noncoding RNA dysregulation in ischemic heart failure. J Transl Med 14: 183, 2016.
28. Yin Q, Wu A and Liu M: Plasma long non-coding RNA (lncRNA) GAS5 is a new biomarker for coronary artery disease. Med Sci Monit 23: 6042-6048, 2017.
29. Lee WS and Kim J: Diabetic cardiomyopathy: Where we are and where we are going. Korean J Intern Med 32: 404-421, 2017.
30. Yang F, Qin Y, Wang Y, Li A, Lv J, Sun X, Che H, Han T, Meng S, Bai Y and Wang L: LncRNA KCNQ1OT1 mediates pyroptosis in diabetic cardiomyopathy. Cell Physiol Biochem 50: 1230-1244, 2018.
31. Li X, Wang H, Yao B, Xu W, Chen J and Zhou X: lncRNA H19/miR-675 axis regulates cardiomyocyte apoptosis by targeting VDAC1 in diabetic cardiomyopathy. Sci Rep 6: 36340, 2016.
32. Zhou X, Zhang W, Jin M, Chen J, Xu W and Kong X: lncRNA MIAT functions as a competing endogenous RNA to upregulate DAPK2 by sponging miR-22-3p in diabetic cardiomyopathy. Cell Death Dis 8: e2929, 2017.
33. Gao L, Wang X, Guo S, Xiao L, Liang C, Wang Z, Li Y, Liu Y, Yao R, Liu Y and Zhang Y: LncRNA HOTAIR functions as a competing endogenous RNA to upregulate SIRT1 by sponging miR-34a in diabetic cardiomyopathy. J Cell Physiol 234: 4944-4958, 2019.
34. Sathishkumar C, Prabu P, Mohan V and Balasubramanyam M: Linking a role of lncRNAs (long non-coding RNAs) with insulin resistance, accelerated senescence, and inflammation in patients with type 2 diabetes. Hum Genomics 12: 41, 2018.
35. Tao S, Chen L, Song J, Zhu N, Song X, Shi R, Ge G and Zhang Y: Tanshinone IIA ameliorates diabetic cardiomyopathy by inhibiting Grp78 and CHOP expression in STZ-induced diabetes rats. Exp Ther Med 18: 729-734, 2019.
36. Varma U, Koutsifeli P, Benson VL, Mellor KM and Delbridge LMD: Molecular mechanisms of cardiac pathology in diabetes-Experimental insights. Biochim Biophys Acta Mol Basis Dis 1864: 1949-1959, 2018.
37. Xie Z, Lau K, Eby B, Lozano P, He C, Pennington B, Li H, Rathi S, Dong Y, Tian R, *et al*: Improvement of cardiac functions by chronic metformin treatment is associated with enhanced cardiac autophagy in diabetic OVE26 mice. Diabetes 60: 1770-1778, 2011.
38. Yamaguchi O: Autophagy in the heart. Circ J 83: 697-704, 2019.
39. Zhang M, Lin J, Wang S, Cheng Z, Hu J, Wang T, Man W, Yin T, Guo W, Gao E, *et al*: Melatonin protects against diabetic cardiomyopathy through Mst1/Sirt3 signaling. J Pineal Res 63: 2017.
40. Paraskevopoulou MD and Hatzigeorgiou AG: Analyzing MiRNA-LncRNA interactions. Methods Mol Biol 1402: 271-286, 2016.
41. Yin G, Zhang B and Li J: miR2213p promotes the cell growth of nonsmall cell lung cancer by targeting p27. Mol Med Rep 20: 604-612, 2019.